5060 *Macromolecules* **2010**, *43*, 5060–5065
DOI: 10.1021/ma100809v

Macromolecules
ARTICLE

Free-Standing Nanomaterials from Block Copolymer Self-Assembly

Damien Quémener,*,† Guilhem Bonniol,† Trang N. T. Phan,‡ Didier Gigmes,‡ Denis Bertin,‡ and André Deratani†

†*Institut Européen des Membranes (UMR 5635, ENSCM-CNRS-UM2), Université Montpellier 2, C.C. 047, Place E. Bataillon, 34095 Montpellier Cedex 05, France, and* ‡*Laboratoire Chimie Provence (UMR-CNRS 6264) - Chimie Radicalaire, Organique et Polymères de Spécialité, Universités d'Aix-Marseille I, II, et III, Campus Saint Jérôme, Case 542, 13397 Marseille Cedex 20, France*

Received November 20, 2009; Revised Manuscript Received April 28, 2010

ABSTRACT: This work presents the preparation of nanomaterials thanks to the assembly of a triblock copolymer P(Sty_{319}-*co*-AN_{262})-*b*-PEO_{795}-*b*-P(Sty_{319}-*co*-AN_{262}). The 3D construction is directed by the assembly of block copolymer micelles prepared *in situ* during the spin-coating of the block copolymer solution. With a solvent system DMF/toluene 50/50, spherical micelles are formed and assembled into a nanoparticle film. The micelle size in the dry state is 50 nm. With a solvent system DMF/toluene 25/75, worm-like micelles (50 nm in diameter) are formed in situ together with "Y-cylinders" and lead to what we called "spider web" films. Micelles are strongly interacting through a dynamic association process between "bridge" and "loop" conformations of the ABA triblock copolymer. When micelles come into contact, some bridges are formed with the two A blocks localized in the heart of two different micelles. The resulting materials show good mechanical properties and enable the preparation of self-standing polymer films.

Introduction

Superassemblies of nanobuilding blocks[1,2] have found many promising applications in photonics,[3−6] electronics[7−9] and sensing[10−14] due to a control of the material architecture at a nanometric level.

The success of nanomaterial design is solely related to the information contained in the heart of the building block. Macrophysical properties like, for example, mechanical strength, macrostructure, surface functionality, or porosity will be directed by the chemical structure, the morphology, and the surface properties of the building block. The construction of such materials requires several steps including the collection of building blocks, their organization and their binding into a permanent material.[1] Several routes have been explored to collect the building blocks, using simple (sedimentation, evaporation, ...) or more complex techniques (biospecific, external force field, ...). The main idea is to bring together the nanobuilding blocks close enough to enable an organization step to occur. The building block collecting is usually concomitant with the organization stage. This second step is eventually completed by a further post-treatment (annealing by solvent vapors, heating, ...) in order to ensure long-range ordering through dynamic optimization. The last step is related to the binding between the building units in order to maintain the global structure and to ensure the best mechanical strength. Again, these organization and binding steps are concomitant as long-range ordering can be reached only when dynamic association and dissociation of the building blocks are controlled.

Amphiphilic block copolymers (BCs) have been extensively used in the past as functional polymers able to control material interfaces. Illustrated in the pioneering work of Fink et al.[15] in photonic crystals, BCs could also served as starting component for nanomaterial preparation. Diblock and triblock[16−20] copolymers have been assembled in bulk giving rise to a large variety of different morphologies. These nanomaterials have a dense internal and superficial structure unless a selective degradation of one block is applied. On the other side, BCs in selective solvent lead to the preparation of core−shell micelles with a dense insoluble core and a diffuse shell partially swollen by the solvent.[21] BC micelles have been used as building blocks in order to prepare one- and two-dimensional polymer nanomaterials.[22−24] However, BC micelles like any other micelles are characterized by dynamic intermicellar chain exchanges which can destabilized the nanomaterials in certain conditions of temperature, concentration or pH.[21] Different strategies have been developed to stabilize the micelle structure like for example cross-linking, chemical reactions, H-bonding, or simply playing with the thermodynamic parameters.

Building three-dimensional polymer nanomaterials is more complex as the final mechanical properties become of primordial importance. With amphiphilic BCs, the micellar stability is ensured by steric repulsion preventing the interpenetration of micelles in sort that the 3D association appears to be unnatural. However, multilayers of block copolymer micelles have been prepared to modify the surface properties of polymer materials in terms of chemical functionality and hierarchical structure.[25] To counteract the repulsion effect, a layer-by-layer assembly between two components has been explored by using hydrogen-bonding[26] or electrostatic attraction.[27−29]

Herein, we report the preparation of stable nanostructured superassemblies in one step from homogeneous solutions of ABA triblock copolymers. The success of this strategy is essentially due to the design of very stable micelles prepared and self-assembled in situ in few seconds by solvent evaporation.

It is known that preparing micelles from ABA triblock copolymers with a solvent system that preferentially dissolves the middle B block yields to a very stable flower-like morphology composed by a large core of the A block and a thin corona of the B block.[30−34] Because of the chance of the A blocks to be located into two different micelle cores, a bridged configuration can be

*To whom correspondence should be addressed. E-mail: damien.quemener@iemm.univ-montp2.fr.

 Published on Web 05/07/2010

Scheme 1. Synthesis of PSAN-*b*-PEO-*b*-PSAN Triblock Copolymer

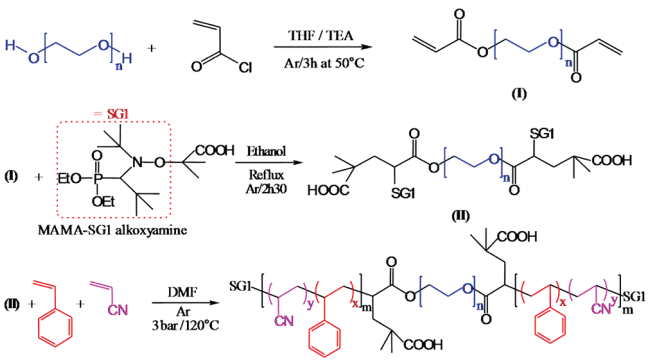

found in addition to the looped conformation. Above a given concentration in micelles, the looped conformation can be switched into the bridged conformation, leading to micelle assembly.[35,36]

In this contribution, the dynamic association properties of flower-like micelles have been explored in order to prepare 3D nanomaterials, through the design of a triblock copolymer poly(styrene-*co*-acrylonitrile)-*b*-poly(ethylene oxide)-*b*-poly(styrene-*co*-acrylonitrile) ($P(Sty_{319}$-*co*-$AN_{262})$-*b*-PEO_{795}-*b*-$P(Sty_{319}$-*co*-$AN_{262})$). The glassy PSAN blocks will enable the formation of compact aggregates constraining the micelles to be kinetically frozen at room temperature, whereas the flexible PEO block will enable the dynamic transitions between looped and bridged chain conformations.

Experimental Part

Synthesis of the Triblock Copolymer. The synthetic procedure of PSAN-*b*-PEO-*b*-PSAN triblock copolymer involves three steps: the preparation of PEO−acrylate (**I**), the intermolecular radical addition of MAMA-SG1 alkoxyamine onto **I** and the copolymerization of styrene and acrylonitrile using macroalkoxyamine based PEO (**II**) as an initiator (Scheme 1).

1. Esterification. PEO−acrylate (**I**) was obtained by esterification of a PEO with a molecular weight of 35000 $g \cdot mol^{-1}$ (Aldrich) with an acryloyl chloride (96%, Aldrich). Typically, in a three-neck round-bottom flask equipped with a water cooled condenser, PEO (20 g) and triethylamine (8 mL) were mixed in 300 mL of tetrahydrofuran. The mixture was then deoxygenated by argon bubbling for 20 min. 4.8 mL of acryloyl chloride was added dropwise under inert atmosphere. After this addition was complete, the solution was heated to 50 °C and the reaction mixture was stirred for 3 h. The solution was then filtered to remove the triethylammonium chloride. Solvent was removed by rotary evaporation at room temperature. The solid was dissolved with 200 mL of CH_2Cl_2 and the solution was washed three times with 20 mL of saturated $NaHCO_3$ solution and three times with 20 mL of distilled water. The product was dried over $MgSO_4$ and the solution was concentrated by rotary evaporation. The saturated solution of PEO−diacrylate was precipitated in cold diethyl ether. It was then filtered, washed with ether and dried under vacuum to a constant weight. The vinyl protons of the acrylate groups in **I** could be observed by ^1H NMR at δ = 6.6−5.7 ppm. The reaction yield of this first step (95 ± 5%) was determined by comparing the integration of these protons peaks and the methylene protons of PEO chain at 3.65 ppm.

2. Intermolecular Radical Addition. A typical procedure for the synthesis of the difunctionnal macroinitiator is the following. In a two-neck round-bottom flask equipped with a water cooled condenser, PEO-diacrylate (15 g) was mixed with 73 mL of ethanol. The alkoxyamine was then added to the solution in excess amount with respect to the acrylate functions (10 equiv). After complete dissolution, the mixture was deoxygenated by nitrogen bubbling for 20 min and then the solution was heated to reflux for 150 min. The solution was then cooled down in iced water and precipitated in cold diethyl ether. It was then filtered, washed with ether, and dried under vacuum to a constant weight. The ^1H NMR spectrum of the macroalkoxyamine-based PEO shows that the signals due to the vinyl protons of the acrylate group (δ = 6.6−5.7 ppm) have disappeared, indicating a 100% yield for this addition reaction.

3. Preparation of Triblock Copolymer. Styrene (22 g), acrylonitrile (6 g), macroalkoxyamine-based PEO (**II**) (95%, M_n = 35 870 g mol^{-1}) (6.38 g), and *N,N*-dimethylformamide (DMF, 28 g) were mixed to generate a solution that contained 55 wt % of monomers and initiator. Targeted molecular weight of PSAN part was 200 000 g mol^{-1}. This solution was added to a pressure stainless steel reactor (Parr Instrument Co.) equipped with a mechanical stirrer. The mixture was degassed by bubbling argon through the gas inlet valve for 25 min at room temperature. After that, argon gas was charged into the reactor at three bars and the reactor was heated to 120 °C. The copolymerization was stopped by quenching the reactor in an ice bath. Block copolymer was purified by precipitation in a large excess of ether/methanol mixture (4/1, v/v), filtered to remove the volatiles and dried under high vacuum at room temperature to a constant weight. Monomer conversion was calculated by gravimetry after elimination of the residual monomers and solvent under reduced pressure and taking into account the amount of macroalkoxyamine-based PEO (**II**) initially introduced. Monomer conversion was 41% at the end of 3 h of polymerization at 120 °C. The ^1H NMR compositional analysis of the final copolymer allows a deduction of the molecular weight of the PSAN block as well as its composition. On the basis of the integration of aromatic protons (at δ = 7− 6.2 ppm) of PS block to the integration of ethylenic protons (δ = 3.4 ppm) of PEO, we have calculated the experimental degree polymerization of PS part. The degree of polymerization of PAN was calculated according to the integration of the signal at 3−0.5 ppm compared to that of ethylenic protons (δ = 3.4 ppm) of PEO. In fact, the peaks in this region correspond at the same time to CH_2 and CH protons of PAN and PS sequences as well as the protons of SG1 moieties. The polymerization degree of PAN sequence is thus calculated by the equation $DP_n(PAN)$ = [Int. (signal at 3−0.5 ppm) − Int. (signal at 7−6.2 ppm) × 3/5 − Int. due to the protons of SG1 moieties]/3, where Int. (signal at 3−0.5 ppm) is the integration of the signal at 3−0.5 ppm and Int. (signal at 7−6.2 ppm) is the integration of aromatic protons at 7−6.2 ppm of PS sequence. According to this estimation, the obtained triblock copolymer has the following composition: $P(Sty_{319}$-*co*-$AN_{262})$-*b*-PEO_{795}-*b*-$P(Sty_{319}$-*co*-$AN_{262})$, the subscripts indicate the degree of polymerization of each polymer part in the triblock copolymer.

Preparation of the Polymer Films. The solutions have been prepared under dry atmospheric conditions by dissolving the triblock copolymer in a DMF/toluene mixture at a concentration of 100 $mg \cdot mL^{-1}$. To prevent any external contaminations, solvents have been added through a syringe fitted with a PTFE filter with a pore diameter of 0.45 μm. The polymer solution is then homogenized under magnetic stirring for 5 days. The silicon wafers were used as small pieces of 1 cm^2. In order to ensure a clean surface, wafers are dipped in a 2 wt % of cleaning surfactant solution (RBS35, Chemical products) under ultrasounds. The wafers are then rinsed with ultrapure water and dipped into heptane flask under ultrasounds. After a second rinse in ultrapure water, the silicon wafers are finally dried under vacuum. The spin coater is first purged under argon at a pressure of 3 bar for 10 min in order to minimize the presence of water. Several droplets of the polymer solution were passed through a PTFE filter with a pore diameter of 5 μm and deposited onto the silicon wafer maintained by vacuum into the spin coater. The spin coater is then turned on at 2000 rpm for 60 s with a speed ramp of 50 $rpm \cdot s^{-2}$. Polymer films were then kept under vacuum for 1 day in order to complete the drying process.

Results and Discussion

Synthesis of the Triblock Copolymer Precursor. The synthetic route of PSAN-*b*-PEO-*b*-PSAN triblock copolymer involves three steps: the preparation of PEO−diacrylate (**I**), the intermolecular radical addition of MAMA-SG1 alkoxyamine onto **I** and the copolymerization of styrene and acrylonitrile using macroalkoxyamine-based PEO (**II**) as an initiator (Scheme 1).

Following a strategy well-described in the literature,[37−41] the addition of the MAMA−SG1 alkoxyamine to the PEO diacrylate (**I**) is carried out via a thermal homolysis of the NO−C bond leading to the formation of the two corresponding radicals and followed by their addition onto the acrylate double bonds. The purified product was obtained with high yield (~85%), and its ^{1}H NMR characterization agreed well with the expected difunctional macroalkoxyamine PEO−(MAMA−SG1)$_2$ structure (Supporting Information, Figure S1). In a second reaction, this PEO-macroinitiator was used to initiate the copolymerization of styrene and acrylonitrile in *N,N*-dimethylformamide (DMF) at 110 °C under a pressure of 3 bar. The reaction mixture became progressively more viscous and remained homogeneous in appearance throughout the polymerization.

The linearity of the relationship of ln([M$_o$]/[M]) versus reaction time for the copolymerization of styrene and acrylonitrile initiated by difunctional PEO macroalkoxyamine (**II**) (Figure 1A) indicates that the number of propagating species remained constant throughout the polymerization. Control over the growth of poly(styrene-*co*-acrylonitrile) chains is furthermore evidenced by the linear evolution of the experimental M_n of PSAN determined by ^{1}H NMR with conversion and a good agreement between experimental M_n and the theoretical values based on conversion (Figure 1B). A clear shift of the SEC traces (Supporting Information, Figure S2) toward higher molecular weights is observed in the course of the polymerization which confirms high initiation efficiency.

We observed an enlargement of SEC chromatograms when monomers conversion reached 40%.This enlargement is due to a small shoulder and to some tailing apparition at the high molecular weight side and the low molecular weight side of the SEC chromatogram, respectively. We attributed the small shoulder to some coupling reactions that were occurring in a very viscous medium or at high monomer conversion, while the tailing was probably coming from the occurrence of some transfer reactions.

According to the ^{1}H NMR spectrum recorded in $CDCl_3$ (not presented here) of the purified product, the obtained PSAN-*b*-PEO-*b*-PSAN triblock copolymer had the following characteristics: PEO sequence (M_n = 35000 g·mol^{-1}, 27.1 wt %), PS sequence (M_n = 66400 g·mol^{-1}, 51.4 wt %) and PAN sequence (M_n = 27800 g·mol^{-1}, 21.5 wt %). In the rest of the article, the appellation P(Sty$_{319}$-*co*-AN$_{262}$)-*b*-PEO$_{795}$-*b*-P(Sty$_{319}$-*co*-AN$_{262}$) will be used; the subscripts indicate the degree of polymerization of each polymer part in the triblock copolymer.

Preparation of Particle Nanomaterial. This superstructure was prepared from a homogeneous solution of PSAN-*b*-PEO-*b*-PSAN in DMF/toluene (50/50 v/v) at a concentration of 100 mg/mL. No micelle could be detected in the solution by Photon Cross Correlation Spectroscopy, even after increasing the concentration up to 200 mg/mL, which seems to indicate a high critical micellar concentration (cmc) in this solvent system. Beyond this concentration, the polymer solution was too viscous to be analyzed. The homogeneous solution of the BC in DMF/Toluene was then spin-coated onto a silicon wafer in order to let the solvent to evaporate.

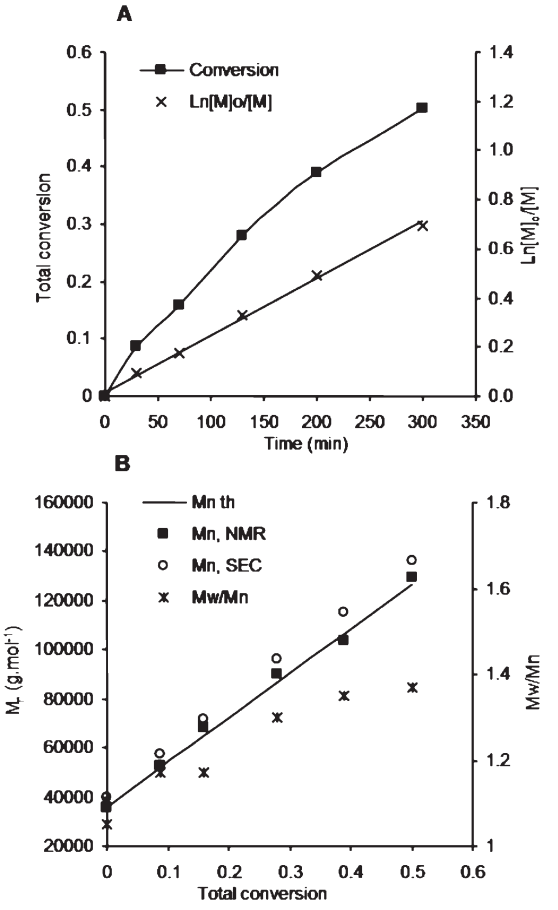

Figure 1. Copolymerization of styrene and acrylonitrile at 110 °C in *N,N*-dimethylformamide (DMF) using the difunctional macroalkoxyamine PEO-(MAMA-SG1)$_2$ (**II**) as initiator. (A) Evolution of monomers conversion and ln([M]$_o$/[M]) versus time data. (B) Evolution of M_n an M_w/M_n with conversion. $M_{n,NMR}$: M_n estimated from the ^{1}H NMR spectra of samples collected from reaction mixture. $M_{n,SEC}$: M_n estimated from SEC chromatograms by using calibration curve established with polystyrene standards.

Atomic force microscopy (AFM) and scanning electron microscopy (SEM) have been carried out in order to characterize the top surface and the cross-section of the nanomaterial (Figure 2). Observation by AFM shows that the film obtained by evaporation from 50/50 v/v DMF/toluene copolymer solution, is composed of nanoparticles with a diameter of about 50 nm and a narrow size distribution as illustrated in Figure 2A. In addition, the film surface is very flat as seen in 3D AFM image (see Supporting Information, Figure S3) with a Z value of about 20 nm—which corresponds approximately to half value of the particle diameter—indicating a dense packing of nanoparticles.

These observations suggest us to propose the following formation mechanism of the nanoparticle film as illustrated in Figure 3.

During the solvent evaporation, the cmc is probably reached (but not observed) and flower-like micelles are formed *in situ*. Indeed, the evaporation step being very fast (i.e., 2 min) and the solution viscous, this intermediate state could not be characterized. We propose that after the appearance of micelles, the solvent evaporation leads to a progressive decrease of the micelle-to-micelle distance. When BC micelles are close enough to interact, dynamic association could take place through bridged conformations of the ABA polymer chains as stated in the literature.[35,36] The in situ preparation of the micelles seems to enable an optimization

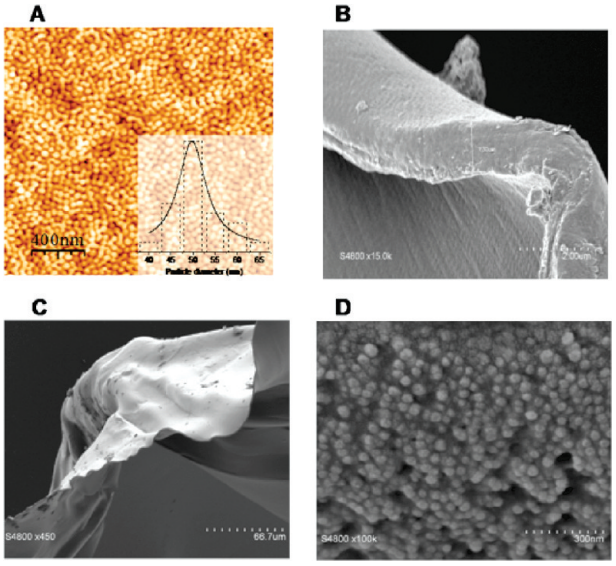

Figure 2. Self-standing nanoparticle superlattice film prepared from a DMF/toluene (50/50, v/v) copolymer solution. (A) AFM top view of the superstructure and size distribution of particle diameter determined by a picture analysis over 100 particles. (B) SEM top, bottom, and cross-sectional view of a stretched nanoparticle film. (C) Crack free stretched nanoparticle film. (D) Enlargement of the cross-section showing a homogeneous nanoparticle morphology.

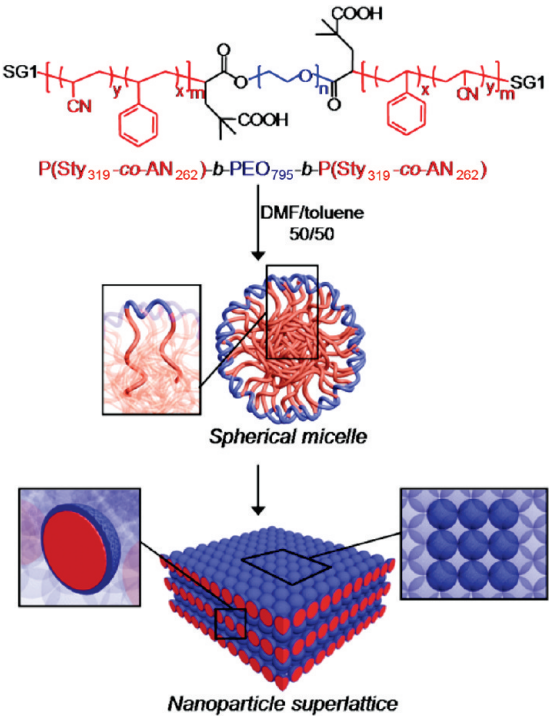

Figure 3. Schematic depiction of the self-assembly of PSAN-*b*-PEO-*b*-PSAN into nanoparticle film.

of the particle packing by delaying the micelle formation at higher polymer concentrations. In order to explore an alternative strategy, we have first solubilized the copolymer in DMF (100 mg·mL^{-1}) followed by a slow addition of water. The addition was stopped at a concentration of 90% of water and the resulting solution was dialyzed against water in order to remove the DMF. In this case, micelles were detected in PCCS in high concentration with a hydrodynamic diameter of 110 nm, which confirms the ability of the BC to be assembled into micellar morphology. This water-based

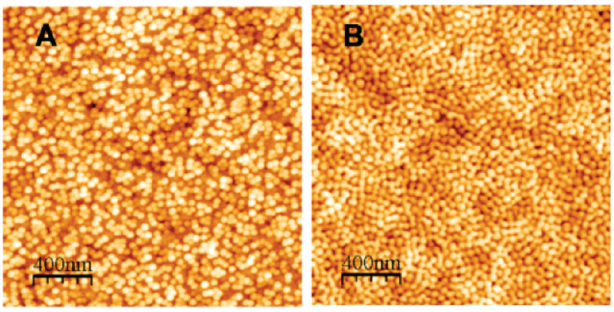

Figure 4. Top surface AFM pictures of nanoparticle films. (A) Micelles produced in DMF/water and then spin coated onto a Si wafer. (B) Micelles produced in situ from DMF/toluene solution during the spin-coating onto a Si wafer.

dispersion of micelles was then spin-coated onto a Si wafer in order to prepare a polymer film. The AFM picture of the film surface (Figure 4A) shows a loose packing with many holes in comparison with the dense packing morphology obtained from the previous in situ strategy (Figure 4B). In conclusion, this alternative strategy seems to be less efficient in terms of particle organization. We propose that during the spin-coating of the water-based dispersion, micelles come into contact with the surface and stay probably at around this place without any efficient dynamic adjustment.

SEM enables us to evidence the apparent good mechanical properties of the superstructure, probably due to the presence of bridged BC conformations. Parts B and C of Figure 2 show that stretching the film can take place without forming cracks. Figure 2D is an enlargement of the cross-section showing a homogeneous particulate structure across the film. Some particles are missing on this picture as the cross section was carried out by breaking the film in liquid nitrogen in such a way that part of the particles located on the same layer remained on the other piece of the film. The film thickness is about 1.3 μm, which corresponds theoretically to 35 layers of particles in case of a perfect hexagonal ordering. Furthermore, the film thickness can be modulated down to 50 nm—which corresponds to a monolayer—by lowering the concentration of the initial polymer solution from 10 to 0.25 wt %.

The water contact angle (WCA) of the nanoparticle film was measured to be 35°, which confirms the presence of hydrophilic PEO on the particle film surface.[42] The hydrophobic PSAN core (WCA = 110° on flat PSAN surface) is "shielded" by the PEO corona in such a way that the surface properties of the material is only related to the thin PEO layer.

It must be mentioned that nanoparticle films can also be observed from BC solutions in pure DMF. However, the reproducibility was poor. We assume that small unwanted changes in the process parameters might switch the organization from nanoparticle to short worm-like superstructure (see Supporting Information, Figure S4). By adding some toluene, the window to target the spherical or the worm-like structure is enlarged and the reproducibility is ensured. On the other hand, disconnected worm-like micelle film with diameter of about 50 nm is observed by AFM when pure toluene was used as solvent (see Supporting Information, Figure S5). Processing is the key step in this strategy and can alter the quality of the material. As an example, by increasing the speed rate of the spin coater, micelles do not have enough time to self-organize through a dynamic process and so rough surface with some failures can be observed (see Supporting Information, Figure S6).

Preparation of "Spider Web" Nanomaterial. As diffusitivity of block copolymers in solution is too small to respond

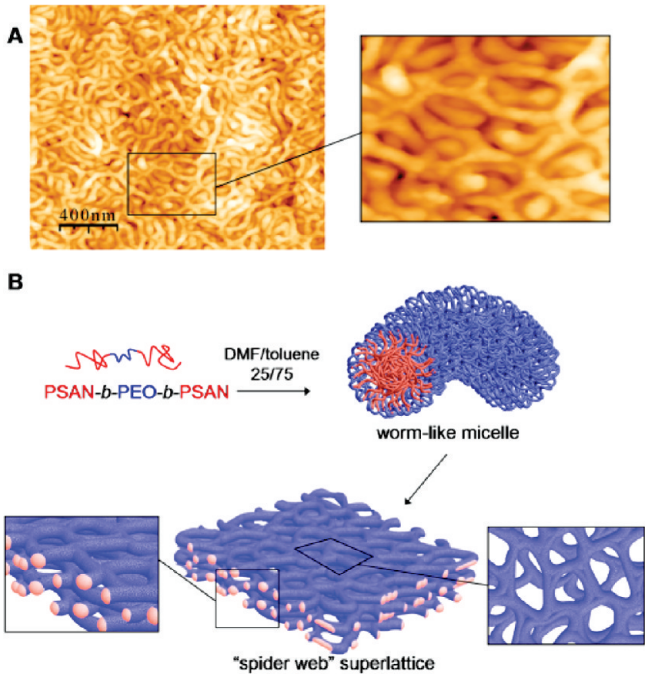

Figure 5. Self-standing "spider web" superlattice film obtained from a DMF/toluene (25/75, v/v) copolymer solution. (A) AFM image of the top surface of the interconnected worm-like micelle network. (B) Schematic depiction of the self-assembly of PSAN-*b*-PEO-*b*-PSAN into a "spider web" superstructure.

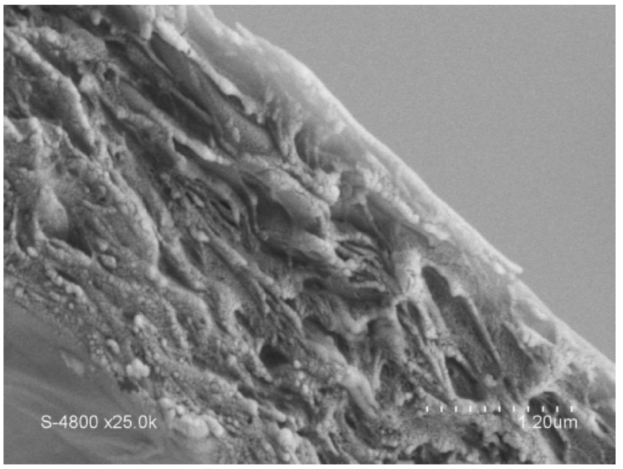

Figure 6. SEM cross-sectional view of the "spider-web" nanomaterial.

to the fast change of solvent concentration and composition during the evaporation stage, the equilibrium micelle morphology is never reached. This lack of overall equilibrium has been previously used to modify the micelle morphology by a change of solvents without changing the block copolymer structure.[43] In our work, by increasing the toluene content from 50 to 75 vol %, a "spider web" superstructure with a highly connected network of worm-like micelles is observed instead of a nanoparticle film (Figure 5A). The worm-like micelles have a diameter of 50 nm and their connections make pores with an average size of 90 nm and a broad pore size distribution.

It has been demonstrated in the past the possibility to prepare "Y-junctions" in a bicomponent system (solvent and surfactant), leading to three-dimensional network of connected worm-like micelles through a macrophase separation mechanism.[44] The change of solvent composition seems to have enabled the formation *in situ* of a percentage of "Y-junctions" high enough to build a 3D network. The SEM picture in Figure 6 represents a cross-sectional view of the spider-web film. The expected 3D porous network seems not to be isotropic, with an organization close to a multilayer system with a preferential 2D construction.

Because of the nanoporous structure, layers are more interpenetrated compared to the nanoparticle film giving rise to a rougher surface with a Z value of about 100 nm. 3D AFM images and large scale image of the "spider web" film is shown in Supporting Information, Figure S7. Figure 5B depicts the proposed formation mechanism of the "spider web" structure. By increasing the toluene content, the shape of the micelles changes from sphere to cylinder probably mixed with "Y-cylinders". During the evaporation stage, micelle concentration increases and some interconnections take place between micelles thanks to the dynamic formation of bridged conformation of the ABA triblock copolymer.

Conclusions

In summary, we demonstrate that the assembly of triblock copolymer (ABA) micelles offers a great potential to prepare nanomaterials. This strategy is based on the dynamic interactions between flower-like micelles, leading to a transition between "loop" and "bridge" conformations of the ABA chain. This bridge conformation enables the formation of self-standing crack free nanostructured film. Initially solubilized in a mixture of DMF and toluene, the triblock copolymer is assembled into micelles during the spin-coating of the solution onto a Si wafer. The evaporation of the solvent enables the micelles to come into contact, followed by the formation of bridge conformations which leads to permanent nanomaterials. By playing with the solvent system, spherical or worm-like micelles are formed in situ and assembled into two different nanomaterials, the nanoparticle and the "spider web" films. This approach opens perspectives to prepare highly engineered nanoporous materials with pore size controlled by the interspaces between particles or by the superposition of "spider web" layers. Their use in membrane technology is currently under progress.

Acknowledgment. The authors grateful acknowledge Michel Ramonda and Didier Cot for their technical assistance in AFM and SEM observations and the support from Agence Nationale de la Recherche (ANR-07-NANO-055).

Supporting Information Available: Supporting Figures S1−S7, showing NMR spectra, SEC chromatograms, and AFM images. This material is available free of charge via the Internet at http://pubs.acs.org.

References and Notes

(1) Velev, O. D.; Gupta, S. *Adv. Mater.* **2009**, *21*, 1897.
(2) Sayle, D. C.; Seal, S.; Wang, Z.; Mangili, B. C.; Price, D. W.; Karakoti, A. S.; Kuchibhatla, S. V. T. N.; Hao, Q.; Mobus, G.; Xu, X.; Sayle, T. X. T. *ACS Nano* **2008**, *2*, 1237.
(3) Braun, P. V.; Wiltzius, P. *Nature* **1999**, *402*, 603.
(4) Blanco, A.; Chomski, E.; Grabtchak, S.; Ibisate, M.; John, S.; Leonard, S. W.; Lopez, C.; Meseguer, F.; Miguez, H.; Mondia, J. P.; Ozin, G. A.; Toader, O.; van Driel, H. M. *Nature* **2000**, *405*, 437.
(5) Joannopoulos, J. D. *Nature* **2001**, *414*, 257.
(6) Vlasov, Y. A.; Bo, X. Z.; Sturm, J. C.; Norris, D. J. *Nature* **2001**, *414*, 289.
(7) Hermanson, K. D.; Lumsdon, S. O.; Williams, J. P.; Kaler, E. W.; Velev, O. D. *Science* **2001**, *294*, 1082.
(8) Amlani, I.; Rawlett, A. M.; Nagahara, L. A.; Tsui, R. K. *Appl. Phys. Lett.* **2002**, *80*, 2761.
(9) Jeong, U.; Teng, X. W.; Wang, Y.; Yang, H.; Xia, Y. N. *Adv. Mater.* **2007**, *19*, 33.

(10) Bezryadin, A.; Dekker, C.; Schmid, G. *Appl. Phys. Lett*. **1997**, *71*, 1273.
(11) Wohltjen, H.; Snow, A. W. *Anal. Chem*. **1998**, *70*, 2856.
(12) Velev, O. D.; Kaler, E. W. *Langmuir* **1999**, *15*, 3693.
(13) Shipway, A. N.; Katz, E.; Willner, I. *Chemphyschem* **2000**, *1*, 18.
(14) Park, S. J.; Taton, T. A.; Mirkin, C. A. *Science* **2002**, *295*, 1503.
(15) Fink, Y.; Urbas, A. M.; Bawendi, M. G.; Joannopoulos, J. D.; Thomas, E. L. *J. Lightwave Technol*. **1999**, *17*, 1963.
(16) Lynd, N. A.; Meuler, A. J.; Hillmyer, M. A. *Prog. Polym. Sci*. **2008**, *33*, 875.
(17) Darling, S. B. *Prog. Polym. Sci*. **2007**, *32*, 1152.
(18) Hadjichristidis, N.; Iatrou, H.; Pitsikalis, M.; Pispas, S.; Avgeropoulos, A. *Prog. Polym. Sci.* **2005**, *30*, 725.
(19) Klok, H.-A.; Lecommandoux, S. *Adv. Mater*. **2001**, *13*, 1217.
(20) Meuler, A. J.; Hillmyer, M. A.; Bates, F. S. *Macromolecules* **2009**, *42*, 7221.
(21) Rodríguez-Hernández, J.; Chécot, F.; Gnanou, Y.; Lecommandoux, S. *Prog. Polym. Sci.* **2005**, *30*, 691.
(22) Cui, H.; Chen, Z.; Zhong, S.; Wooley, K. L.; Pochan, D. J. *Science* **2007**, *317*, 647.
(23) Kim, T. H.; Huh, J.; Hwang, J.; Kim, H. -C.; Kim, S. H.; Sohn, B.-H.; Park, C. *Macromolecules* **2009**, *42*, 6688.
(24) Tu, Y.; Graham, M. J.; Van Horn, R. M.; Chen, E.; Fan, X.; Chen, X.; Zhou, Q.; Wan, X.; Harris, F. W.; Cheng, S. Z. D. *Polymer* **2009**, *50*, 5170.
(25) Zhao, N.; Zhang, X. Y.; Zhang, X. L.; Xu, J. *Chemphyschem* **2007**, *8*, 1108.
(26) Kim, B.-S.; Park, S. W.; Hammond, P. T. *ACS Nano* **2008**, *2*, 386.
(27) Cho, J.; Hong, J.; Char, K.; Caruso, F. *J. Am. Chem. Soc*. **2006**, *128*, 9935.
(28) Sakai, K.; Webber, G. B.; Vo, C.-D.; Wanless, E. J.; Vamvakaki, M.; Bütün, V.; Armes, S. P.; Biggs, S. *Langmuir* **2008**, *24*, 116.
(29) Sharma, V.; Yan, Q.; Wong, C. C.; Carter, W. C.; Chiang, Y.-M. *J. Colloid Interface Sci.* **2009**, *333*, 230.
(30) Riegel, I. C.; Eisenberg, A.; Petzhold, C. L.; Samios, D. *Langmuir* **2002**, *18*, 3358.
(31) Riegel, I. C.; de Bittencourt, F. M.; Terrau, O.; Eisenberg, A.; Petzhold, C. L.; Samios, D. *Pure Appl. Chem*. **2004**, *76*, 123.
(32) Walther, A.; Goldmann, A. S.; Yelamanchili, R. S.; Drechsler, M.; Schmalz, H.; Eisenberg, A.; Muller, A. H. E. *Macromolecules* **2008**, *41*, 3254.
(33) Zhang, L. F.; Eisenberg, A. *J. Am. Chem. Soc*. **1996**, *118*, 3168.
(34) Zhang, L. F.; Eisenberg, A. *Macromolecules* **1999**, *32*, 2239.
(35) Giacomelli, F. C.; Riegel, I. C.; Petzhold, C. L.; da Silveira, N. P.; Stepanek, P. *Langmuir* **2009**, *25*, 731.
(36) Giacomelli, F. C.; Riegel, I. C.; Petzhold, C. L.; da Silveira, N. P.; Stepanek, P. *Langmuir* **2009**, *25*, 3487.
(37) Robin, S.; Guerret, O.; Couturier, J. L.; Pirri, R.; Gnanou, Y. *Macromolecules* **2002**, *35*, 3844.
(38) Nicolas, J.; Charleux, B.; Guerret, O.; Magnet, S. *Macromolecules* **2005**, *38*, 9963.
(39) Dufils, P.-E.; Chagneux, N.; Gigmes, D.; Trimaille, T.; Marque, S. R. A.; Bertin, D.; Tordo, P. *Polymer* **2007**, *48*, 5219.
(40) Clement, B.; Trimaille, T.; Alluin, O.; Gigmes, D.; Mabrouk, K.; Feron, F.; Decherchi, P.; Marqueste, T.; Bertin, D. *Biomacromolecules* **2009**, *10*, 1436.
(41) Bloch, E.; Phan, T.; Bertin, D.; Llewellyn, P.; Hornebecq, V. *Microporous Mesoporous Mater*. **2008**, *112*, 612.
(42) Miqin, Z.; Desai, T.; Ferreri, M. *Biomaterials* **1998**, *19*, 953.
(43) Cui, H. G.; Chen, Z. Y.; Zhong, S.; Wooley, K. L.; Pochan, D. J. *Science* **2007**, *317*, 647.
(44) Jain, S.; Bates, F. S. *Science* **2003**, *300*, 460.